

QPO frequencies and mass-outflow rates in black hole powered galactic microquasars

Tapas K. Das ^{1,2,3} A. R. Rao ⁴ Santosh V. Vadawale ⁴

¹ Division of Astronomy, Department of Physics and Astronomy, University of California at Los Angeles, Box 951562, Los Angeles, CA 90095-1562, USA

² Institute of Geophysics and Planetary Physics, University of California at Los Angeles, Box 951567, Los Angeles, CA 90095, USA

³ Racah Institute of Physics, The Hebrew University, Jerusalem 91405, Israel

⁴ Tata Institute of Fundamental Research, Homi Bhabha Road, Mumbai 400005, India

tapas@astro.ucla.edu, arrao@tifr.res.in, santoshv@tifr.res.in

Accepted . Received ; in original form

ABSTRACT

For all available pseudo-Schwarzschild potentials, we provide a non-self-similar model of coupled accretion-outflow system in connection to the Quasi Periodic Oscillation (QPO) of the black hole powered galactic microquasars and the emergence of barionic jets out of these objects. We use the vertically integrated 1.5 dimensional model to describe the disc structure where the equations of motion are written on the equatorial plane of the central accretor, assuming the flow to be in hydrostatic equilibrium in the transverse direction. First we formulate and solve the equations governing axisymmetrically rotating, advective, multi-transonic black hole accretion which may contain the Rankine Hugoniot Shock Waves (RHSW), and then we calculate the associated QPO frequencies ν_{QPO} in terms of relevant accretion parameters. We then argue that the post-shock region for such flows may serve as an efficient source of outflow generation; and we calculate, for *same* set of accretion parameters used to calculate the ν_{QPOs} , what fraction of the accreting material, denoted by R_{in} , is being blown as shock generated outflow. In this way we theoretically study the relation between ν_{QPOs} and R_{in} for galactic microquasars and compare our theoretically obtained result with observational data.

Key words: Accretion, accretion discs — black hole physics — hydrodynamics — stars — winds — outflows — x-rays: stars

To Appear in the Monthly Notices of Royal Astronomical Society (MNRAS)

1 INTRODUCTION

It has been established in recent years that in order to satisfy the inner boundary conditions imposed by the event horizon, accretion onto black holes should exhibit transonic properties in general; which further indicates that formation of shock waves are possible in astrophysical fluid flows onto galactic and extra-galactic black holes. One also expects that shock formation in black hole accretion might be a general phenomena because shock waves in rotating and non-rotating flows are convincingly able to provide an important and efficient mechanism for conversion of significant amount of the gravitational energy (available from deep potential wells created by these massive compact accretors) into radiation by randomizing the directed infall motion of the accreting fluid. Hence shocks possibly play an important role in governing the overall dynamical and radiative processes taking place in astrophysical fluid and plasma accreting onto black holes. Thus the study of steady, standing, stationary shock waves produced in black hole accretion has acquired a very important status in recent years and it is now believed that shocks may be an important ingredient in an accreting black hole system in general (for an extended list of literatures on shock formation in black hole accretion, see Das 2002, D02 hereafter, and references therein). Hot, dense and exo-entropic post-shock regions in advective accretion disks are also used as a powerful tool in understanding the spectral properties of black hole candidates (Shrader & Titarchuk 1998, and references therein) and in theoretically explaining a number of diverse phenomena, including the generation mechanism for high frequency Quasi Periodic Oscillations (QPOs) in general (Titarchuk, Lapidus & Muslimov 1998, and references therein). A number of observational evidences are also present which are in close agreement with the theoretical predictions obtained from shocked accretion model (Rutledge et al. 1999;

Muno, Morgan & Remillard 1999; Webb & Malkan 2000; Rao, Yadav & Paul 2000; Smith, Heindl & Swank 2001). In their attempt to explain some of the observational features of galactic microquasars, Chakrabarti & Manickam (Chakrabarti & Manickam 2000) proposed that the intermediate frequency ($\nu \sim 1 - 10\text{Hz}$) and high frequency QPO of the black hole candidate (harbored by GRS 1915+105) may occur due to oscillations of shocks in accretion disc. In a recent work, Das (2003, hereafter D03), showed that the QPOs in galactic sources are, *indeed*, regulated by shocked accretion flow, and analytically calculated the QPO frequency as a function of fundamental accretion parameters. It is now a well established fact that quasars and microquasars suffer mass loss through outflows and jets (Mirabel & Rodriguez 1999; Ferrari 1998; Begelman, Blandford & Rees 1984). These galactic and extra-galactic jet sources are commonly believed to harbor accreting compact objects at their hearts as the prime movers for almost all non stellar energetic activities around them including the production of bipolar outflows and relativistic jets. Unlike normal stellar bodies, compact objects do not have their own physical atmosphere from where matter could be ripped off as winds, hence outflows from the vicinity of these prime movers have to be generated only from the accreting material. So instead of separately investigating the jets and accretion processes as two disjoint issues around the dynamical center of the galactic and extra-galactic jet sources, it is very necessary to study these two phenomena within the same framework and any consistent theoretical model for jet production should explore the outflow formation only from the knowledge of accretion parameters. Also to be noted that while self-similar models are a valuable first step, they can never be the full answer, and indeed any model which works equally well at all radii is fairly unsatisfactory to prove its viability. Thus the preferred model for jet formation must be one which is able to select the specific region of jet formation. Motivated by the above mentioned arguments, Das (Das 1998, D98 hereafter, Das 2001) and Das & Chakrabarti (Das & Chakrabarti 1999, DC hereafter) proposed a non self-similar analytical model capable of self-consistently exploring the hydrodynamic origin of accretion powered jets/outflows emanating out from galactic and extra-galactic sources. D98 and DC computed mass outflow rates from accretion disks around compact objects, such as neutron stars and black holes. These computations were done using combinations of exact transonic inflow and outflow solutions which may form standing shock waves. Assuming that the bulk of the outflow is from the shock generated effective boundary layers of these objects, they found that the ratio of the outflow rate to the inflow rate varies anywhere from a few percent to even close to a hundred percent (i.e., close to disk evacuation case) depending on the initial parameters of the disk, the degree of compression of matter near the centrifugal barrier, and the polytropic index of the flow. Also the exact location (distance measured from the central accretor) of the jet launching zone has been successfully pointed out in their work.

Since D98, D03 and DC share a common underlying phenomena, the formation of steady, standing Rankine Hugoniot shock waves (RHSW hereafter) in a thin, rotating, axisymmetric, inviscid steady accretion flow around black holes, we believe that it is worth investigating whether theoretical calculations allows one to correlate the frequencies of QPO of a black hole candidate with the amount of barionic content of jets emanating from the vicinity of that black hole sitting at the heart of any galactic microquasar, and if so, whether such theoretical correlation may further be supported by present day observational evidences. Our approach in this paper is precisely this. First we formulate and solve the equations governing axisymmetrically rotating, multi-transonic inviscid black hole accretion which may contain RHSW and then we calculate the associated QPO frequencies ν_{QPO} in terms of relevant accretion parameters. We then argue that the post-shock region for such flows may serve as an efficient source of outflow generation and we calculate, for the *same* set of accretion parameters used to calculate the ν_{QPO} , what fraction of the accreting material, denoted by $R_{\dot{m}}$, is being blown as shock generated wind. Ultimately we provide the correlation among ν_{QPO} s and $R_{\dot{m}}$ s and check the feasibility of our theoretically obtained result against observational data.

2 INFLOW EQUATIONS, MULTIPLICITY OF SONIC POINTS AND SHOCK FORMATION

Rigorous investigation of the complete general relativistic multi-transonic black hole accretion disc and wind is believed to be extremely complicated. At the same time it is understood that as relativistic effects play an important role in the regions close to the accreting black hole (where most of the gravitational potential energy is released), purely Newtonian gravitational potential (in the form $\Phi_N = -\frac{GM_{BH}}{r}$, where M_{BH} is the mass of the compact accretor) cannot be a realistic choice to describe transonic black hole accretion in general. To compromise between the ease of handling of a Newtonian description of gravity and the realistic situations described by complicated general relativistic calculations, a series of ‘modified’ Newtonian potentials have been introduced to describe the general relativistic effects that are most important for accretion disk structure around Schwarzschild and Kerr black holes. Introduction of such potentials allows one to investigate the complicated physical processes taking place in disc accretion in a semi-Newtonian framework by avoiding pure general relativistic calculations so that most of the features of spacetime around a compact object are retained and some crucial properties of the analogous relativistic solutions of disc structure could be reproduced with high accuracy. Hence, those potentials might be designated as ‘pseudo-Kerr’ or ‘pseudo-Schwarzschild’ potentials, depending on whether they are used to mimic the space time around a rapidly rotating or non rotating/ slowly rotating (Kerr parameter $a \sim 0$) black hole respectively.

It is important to note that as long as one is not interested in astrophysical processes extremely close (within $1 - 2 r_g$) to a black hole horizon, one may safely use these black hole potentials to study accretion on to a Schwarzschild black hole with the advantage that use of these potentials would simplify calculations by allowing one to use some basic features of flat geometry (additivity of energy or de-coupling of various energy components etc.) which is not possible for calculations in a purely Schwarzschild metric. Also, one can study more complex many body problems such as accretion from an ensemble of companions or overall efficiency of accretion onto an ensemble of black holes in a galaxy or for studying numerical hydrodynamic

accretion flows around a black hole etc. as simply as can be done in a Newtonian framework, but with far better accuracy. However, one should be careful in using these potentials to study shocked black hole accretion because of the fact that none of the potentials discussed here are ‘exact’ in a sense that they are not directly derivable from the Einstein equations. These potentials could only be used to obtain more accurate correction terms over and above the pure Newtonian results and any ‘radically’ new results obtained using these potentials should be cross-checked very carefully with the exact general relativistic theory.

Our calculations in this paper are based on four such pseudo Schwarzschild potentials. Explicit forms of those four potentials are the following (see Das & Sarkar 2001 and D02 references therein for detail discussion about various properties of these potentials):

$$\begin{aligned}\Phi_1(r) &= -\frac{1}{2(r-1)}; \quad \Phi_2(r) = -\frac{1}{2r} \left[1 - \frac{3}{2r} + 12 \left(\frac{1}{2r} \right)^2 \right] \\ \Phi_3(r) &= -1 + \left(1 - \frac{1}{r} \right)^{\frac{1}{2}}; \quad \Phi_4(r) = \frac{1}{2} \ln \left(1 - \frac{1}{r} \right)\end{aligned}\quad (1)$$

where r is the radial co-ordinate scaled in units of Schwarzschild radius. Hereafter, we will define the Schwarzschild radius r_g as

$$r_g = \frac{2GM_{BH}}{c^2}$$

(where M_{BH} is the mass of the black hole, G is universal gravitational constant and c is velocity of light in vacuum) so that the marginally bound circular orbit r_b and the last stable circular orbit r_s take the values $2r_g$ and $3r_g$ respectively for a typical Schwarzschild black hole. Also, total mechanical energy per unit mass on r_s (sometimes called ‘efficiency’ e) may be computed as -0.057 for this case. We will use a simplified geometric unit throughout this paper where radial distance r is scaled in units of r_g , radial dynamical velocity u and polytropic sound speed a of the flow is scaled in units of c (the velocity of light in vacuum), mass m is scaled in units of M_{BH} and all other derived quantities would be scaled accordingly. For simplicity, we will use $G = c = 1$.

Among the above potentials, $\Phi_1(r)$ was introduced by Paczyński and Wiita (1980) which accurately reproduces the positions of r_s and r_b . Also the Keplerian distribution of angular momentum obtained using this potential is exactly same as that obtained in pure Schwarzschild geometry. $\Phi_2(r)$ was proposed by Nowak and Wagoner (1991) to approximate some of the dominant relativistic effects of the accreting black hole (slowly rotating or non-rotating) via a modified Newtonian potential. It has the correct form of r_s as well as it produces the best approximation for the value of the angular velocity Ω_s (as measured at infinity) at r_s and the radial epicyclic frequency κ (for $r > r_s$). $\Phi_3(r)$ and $\Phi_4(r)$ were proposed by Artemova, Björnsson & Novikov 1996, ABN hereafter, to produce exactly the same value of the free-fall acceleration of a test particle at a given value of r as is obtained for a test particle at rest with respect to the Schwarzschild reference frame (Φ_3) and to produce the value of the free fall acceleration that is equal to the value of the covariant component of the three dimensional free-fall acceleration vector of a test particle that is at rest in the Schwarzschild reference frame (Φ_4) respectively. Hereafter, we will denote any i th potential as $\Phi_i(r)$ where $\{i = 1, 2, 3, 4\}$ corresponds to $\{\Phi_1(r), \Phi_2(r), \Phi_3(r), \Phi_4(r)\}$ respectively.

Following standard literature, we consider a thin, rotating, axisymmetric, inviscid steady flow in hydrostatic equilibrium in transverse direction. The assumption of hydrostatic equilibrium is justified for a thin flow because for such a flow, the infall time scale is expected to exceed the local sound crossing time scale in the direction transverse to the flow. The flow is also assumed to possess considerably large radial velocity which makes the flow ‘advective’ (see D02, and references therein). The complete solutions of such a system (which may allow RHSW to form) require the dimensionless equations for conserved specific energy \mathcal{E} and angular momentum λ of the accreting material and the mass conservation equations supplied by the transonic conditions at the sonic points and the Rankine Hugoniot conditions at the shock. The local half-thickness, $h_i(r)$ of the disc for any Φ_i can be obtained by balancing the gravitational force by pressure gradient and can be expressed as:

$$h_i(r) = a \sqrt{r / (\gamma \Phi'_i)} \quad (2),$$

Φ'_i is the derivative of any i th potential with respect to the radial co-ordinate. For a non-viscous flow obeying the polytropic equation of state $p = K\rho^\gamma$ (K is a measure of the specific entropy of the flow), integration of radial momentum equation:

$$u \frac{du}{dr} + \frac{1}{\rho} \frac{dp}{dr} + \frac{d}{dr} [\Phi_i^{eff}(r)] = 0$$

where $\Phi_i^{eff}(r)$ is the i th ‘effective’ potential which is the summation of the gravitational potential and the centrifugal potential for matter accreting under the influence of i th pseudo potential:

$$\Phi_i^{eff}(r) = \Phi_i(r) + \frac{\lambda^2}{2r^2},$$

leads to the following energy conservation equation in steady state:

$$\mathcal{E} = \frac{1}{2} u_e^2 + \frac{a_e^2}{\gamma - 1} + \frac{\lambda^2}{2r^2} + \Phi_i(r) = 0; \quad (3a)$$

Similarly, the continuity equation:

$$\frac{d}{dr} [u \rho r h_i(r)] = 0$$

can be integrated to obtain the barion number conservation equation as:

$$\dot{M} = \sqrt{\frac{1}{\gamma} u_e a_e \rho_e r^{\frac{3}{2}} (\Phi'_i)^{-\frac{1}{2}}}. \quad (3b)$$

Following standard literature, one can define the entropy accretion rate $\dot{\mathcal{M}} = \dot{M} K^{\left(\frac{1}{\gamma-1}\right)} \gamma^{\left(\frac{1}{\gamma-1}\right)}$ which undergoes a discontinuous transition at the shock location r_{sh} where local turbulence generates entropy to increase $\dot{\mathcal{M}}$ for post-shock flows. For our purpose, explicit expression for $\dot{\mathcal{M}}$ can be obtained as:

$$\dot{\mathcal{M}} = \sqrt{\frac{1}{\gamma} u_e a_e \left(\frac{\gamma+1}{\gamma-1}\right) r^{\frac{3}{2}} (\Phi'_i)^{-\frac{1}{2}}}. \quad (3c)$$

In Eqs. (3a-3c), the subscript e indicates the values measured on the equatorial plane of the disk; however, we will drop e hereafter if no confusion arises in doing so.

At this point, we would like to discuss in detail about some of the assumptions made in this work to study the disc structure and dynamics. Firstly, our calculations are essentially based on inviscid accretion whereas in reality one may expect that viscosity is present in accretion disc around black holes. The exact expression of λ in eq. (8a) may, thus be $\lambda(r)$ (which means that the angular momentum would be a function of the radial distance) and along with the radial momentum equation and continuity equation, two other equations, namely, equations for azimuthal angular momentum and the equation for heating and cooling factors describing the radiative properties of the flow, should be used to bring the whole picture into focus. However, we try to justify our assumption of inviscid flow in the following way:

We will mainly concentrate in a region of accretion disc close to the central accretor (a few Schwarzschild radii away from the event horizon). This is because, except for a few unusual situations, for all reasonable initial boundary conditions for flow in every Φ_i , shocks are likely to form in this length scale (see DO2). Close to the black hole at that length scale, the radial velocity of matter becomes enormously large due to extremely strong gravitational attraction of the black hole, hence infall time scale becomes much smaller compared to the viscous time scale for all practical purposes. So, one can treat the angular momentum to be practically constant irrespective of the nature of viscosity in accretion disc and our assumption of inviscid flow may not be quite unjustified. Nevertheless, one limitation of our model is to treat the flow to be inviscid even at far field position, i.e., at a long distance away from the accretor where the viscous dissipation of angular momentum may be taken into account. We thus, were unable to prescribe any analytical means using which we could smoothly join the far field high viscous flow with near field weakly viscous / practically inviscid flow. However, even thirty years after the discovery of standard accretion disc theory (Shakura & Sunyaev 1973), exact modeling of viscous multi-transonic black hole accretion, including proper heating and cooling mechanism is quite an arduous task, and we do not attempt it in this paper. However, our qualitative calculations show that the introduction of viscosity via a radius dependent power law distribution for angular momentum only weakness the strength of the centrifugal barrier and pushes the shock location closer to the event horizon, keeping the overall basic physics concerning the shock dynamics and related issues unaltered; details of this work is in progress and will be discussed elsewhere.

One can simultaneously solve Eqs. (3a-3c) for any particular Φ_i and for a particular set of values of $\{\mathcal{E}, \lambda, \gamma\}$. Hereafter we will use the notation $[\mathcal{P}_i]$ for a set of values of $\{\mathcal{E}, \lambda, \gamma\}$ for any particular Φ_i .

For a particular $[\mathcal{P}_i]$, it is now quite straight-forward to derive the space gradient of dynamical flow velocity $\left(\frac{du}{dr}\right)_i$ for flow in any particular i th black hole potential $\Phi_i(r)$ as:

$$\left(\frac{du}{dr}\right)_i = \frac{\left(\frac{\lambda^2}{r^3} + \Phi'_i(r)\right) - \frac{a^2}{\gamma+1} \left(\frac{3}{r} + \frac{\Phi''_i(r)}{\Phi'_i(r)}\right)}{u - \frac{2a^2}{u(\gamma+1)}} \quad (4a)$$

Since the flow is assumed to be smooth everywhere, if the denominator of eqn. (4a) vanishes at any radial distance r , the numerator must also vanish there to maintain the continuity of the flow. One therefore arrives at the so called ‘sonic point’ (alternately, the ‘critical point’) conditions’ by simultaneously making the numerator and denominator of eqn. (4a) equal to zero. The sonic point conditions then can be expressed as:

$$a_s^i = \sqrt{\frac{1+\gamma}{2}} u_s^i = \sqrt{\left[\frac{\Phi'_i(r) + \gamma \Phi'_i(r)}{r^2} \left(\frac{\lambda^2 + r^3 \Phi'_i(r)}{3\Phi'_i(r) + r\Phi''_i(r)} \right) \right]_s} \quad (4b)$$

where the subscript s indicates that the quantities are to be measured at the sonic point(s) and Φ''_i represents the derivative of Φ'_i . For a fixed $[\mathcal{P}_i]$ and Φ_i , one can solve the following polynomial of r to obtain the sonic point(s) of the flow where the subscript s refers to the quantities measured at the sonic points:

$$\mathcal{E} - \left(\frac{\lambda^2}{2r^2} + \Phi_i \right)_s - \frac{2\gamma}{\gamma^2 - 1} \left[\frac{\Phi'_i(r) + \gamma \Phi'_i(r)}{r^2} \left(\frac{\lambda^2 + r^3 \Phi'_i(r)}{3\Phi'_i(r) + r\Phi''_i(r)} \right) \right]_s = 0. \quad (4c)$$

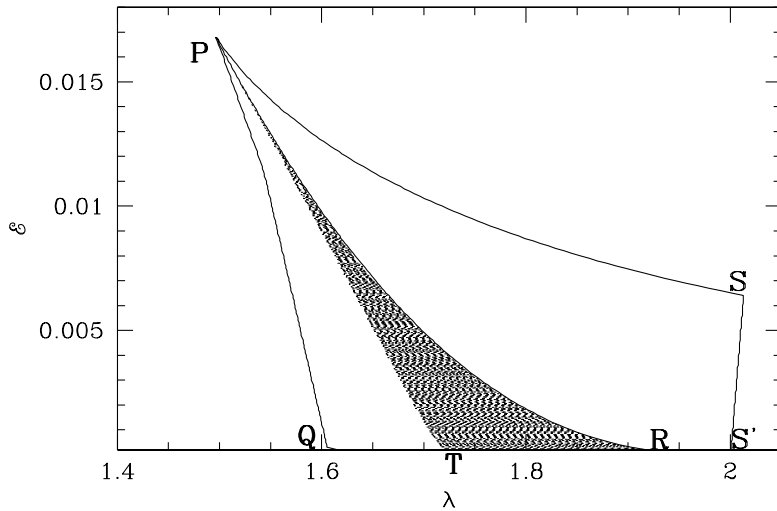


Fig. 1: Classification of parameter space for multi-transonic accretion and wind. Shock formation region is shown for accretion only and not for wind. See text for details.

Similarly, the value of $(\frac{du}{dr})_i$ at its corresponding sonic point(s) r_s^i can be obtained by solving the following equation:

$$\begin{aligned} & \frac{4\gamma}{\gamma+1} \left(\frac{du}{dr} \right)_{s,i}^2 - 2u_s \left(\frac{\gamma-1}{\gamma+1} \right) \left(\frac{3}{r} + \frac{\Phi_i''(r)}{\Phi_i'(r)} \right)_s \left(\frac{du}{dr} \right)_{s,i} \\ & + a_s^2 \left[\frac{\Phi_i'''(r)}{\Phi_i'(r)} - \frac{2\gamma}{(1+\gamma)^2} \left(\frac{\Phi_i''(r)}{\Phi_i'(r)} \right)^2 + \frac{6(\gamma-1)}{\gamma(\gamma+1)^2} \left(\frac{\Phi_i''(r)}{\Phi_i'(r)} \right) - \frac{6(2\gamma-1)}{\gamma^2(\gamma+1)^2} \right]_s \\ & + \Phi_i'' \Big|_s - \frac{3\lambda^2}{r_s^4} = 0 \end{aligned} \quad (4d)$$

Where the subscript “ s, i ” indicates that the corresponding quantities for any i th potential is being measured at its corresponding sonic point(s) and $\Phi_i'''(r) = \frac{d^3\Phi_i(r)}{dr^3}$.

For all Φ_i ’s, we find a significant region of parameter space spanned by $[\mathcal{P}_i]$ which allows the multiplicity of sonic points for accretion as well as for wind where two real physical inner and outer (with respect to the black hole location) X type sonic points r_{in} and r_{out} encompass one O type unphysical middle sonic point r_{mid} in between them. If shock forms in accretion (in this work we will not study the shock formation in wind), then $[\mathcal{P}_i]$ ’s responsible for shock formation must be somewhere from the region for which three sonic points will form in *accretion only*, though not all $[\mathcal{P}_i]$ ’s in the region of multi-transonic accretion will allow shock transition (see subsequent discussions and Fig. 1). Using Eqs. (2,3a-3c), one can combine the three standard RH conditions (Landau & Lifshitz 1959) for vertically integrated pressure and density to derive the following relation which is valid *only* at the shock location:

$$(1-\gamma) \left(\frac{\rho_- \dot{\mathcal{M}}_-}{\dot{M}} \right)^{\log_1^{\Gamma-\Theta}} \mathcal{E}_{(ki+th)} - \Theta(1+\Theta - R_{comp})^{-1} + (1+\Theta)^{-1} = 0, \quad (5)$$

where $\mathcal{E}_{(ki+th)}$ is the total specific thermal plus mechanical energy of the accreting fluid: $\mathcal{E}_{(ki+th)} = [\mathcal{E} - \left(\frac{\lambda^2}{2r^2} + \Phi_i \right)]$, R_{comp} and β are the density compression and entropy enhancement ratio respectively, defined as $R_{comp} = (\rho_+/\rho_-)$ and $\beta = (\dot{\mathcal{M}}_+/\dot{\mathcal{M}}_-)$ respectively; $\Theta = 1 - \Gamma^{(1-\gamma)}$ and $\Gamma = \beta R_{comp}$, “+” and “-” refer to the post- and pre-shock quantities. The shock strength \mathcal{S}_i (ratio of the pre- to post-shock Mach number of the flow) can be calculated as:

$$\mathcal{S}_i = R_{comp} (1 + \Theta). \quad (6)$$

One can simultaneously solve Eqs. (3a-3c,5-6) to find out the shock location r_{sh} along with any sonic or shock quantity as a function of $[\mathcal{P}_i]$ and can identify the regions of parameter space (spanned by \mathcal{E} , λ and γ) responsible for shock formation for any $\Phi_i(r)$. However, one can show that as far as the shock formation in multi-transonic accretion flows around black holes are concerned, the Paczyński and Wiita potential is expected to be the best approximation of complete general relativistic

solutions (D02), and hence, although we will provide a general solution scheme for shock induced outflow for *all* pseudo potentials, we will present our main results for accretion in $\Phi_1(r)$ only.

In Fig. 1, we classify the parameter space for multi-transonic accretion and wind for flows in $\Phi_1(r)$. The specific energy \mathcal{E} is plotted along the Y axis and the specific angular momentum λ is plotted along the X axis. In the region bounded by **PQR**, three sonic points are formed in *accretion*, while three sonic points in *wind* are formed in the region bounded by **PRS'S**. The shaded wedge **PTR** represents the region of parameter space for which multi-transonic accretion flow will have a steady, standing RSHW. Any region which falls outside **PQS'S**, will produce a mono-transonic accretion, so to say. Although the figure is drawn for ultra-relativistic ^{*} flow, one can easily explore multi-transonic shocked accretion flow with higher values of γ ($4/3 < \gamma < 5/3$). For any $[\mathcal{P}_i] \in \mathbf{PTR}$, one can calculate the shock location r_{sh} and the shock compression ratio R_{comp} . Following D03, one can calculate the QPO frequency ν_{QPO} as:

$$\nu_{QPO} = \frac{\mathcal{A}}{R_{comp} r_{sh}^{\frac{3}{2}}} \quad (7)$$

The dimensionless constant \mathcal{A} in the above equation can be determined by scaling the calculated QPO frequencies with the highest possible *observed* ν_{QPO} for a particular astrophysical source.

3 GENERATION OF SHOCK-INDUCED OUTFLOW AND ITS GOVERNING EQUATIONS

The simplicity of black holes lie in the fact that they do not have atmospheres. But the advective accretion discs surrounding them have, and similar method as employed in stellar atmospheres should be applicable to the disks. Our approach in this section is precisely this. We first explain how the post shock region is expected to produce outflows; in doing so we will follow more or less the same arguments used by D98 and DC. Then we will formulate the equations governing such outflows in a general format so that we will incorporate all pseudo potentials. Finally we will simultaneously solve the equations governing the inflow and outflow to find out what fraction of the accreting material, denoted by $R_{\dot{m}}$, is being blown as wind and for the *same* set of accretion parameters, we will correlate that fractional amount with the frequencies of the QPO. Due to the fact that close to the black hole the radial component of the infall velocity of accreting material would be enormously high, viscous time scale would be much longer than the infall time scale and a rotating inflow entering into a black hole will have almost constant specific angular momentum close to the black hole for any moderate viscous stress. This almost constant angular momentum produces a very strong centrifugal force which increases much faster compared to the gravitational force and becomes comparable at some specific radial distance. Here, (actually, a little farther out, due to thermal pressure) matter starts piling up and produces the centrifugal pressure supported boundary layer (CENBOL). Further close to the black hole, the gravity always wins and matter enters the horizon supersonically after passing through a sonic point. Formation of CENBOL may be attributed to the shock formation in accreting fluid. In CENBOL region the post-shock flow becomes hotter and denser and for all practical purposes behaves as the stellar atmosphere so far as the formation of outflows are concerned. A part of the hot and dense shock-compressed inflowing material is then ‘squirt’ as outflow from the CENBOL. Subsonic outflows originating from CENBOL would pass through outflow sonic points and reach far distances as in wind solution. It is to be noted here that the generation of outflow from CENBOL in this work is a rational assumption. The exact analytical calculation describing the change of linear momentum of the accreting material in a direction perpendicular to the plane of the disc is beyond the frame work of the 1.5 dimensional disc model used in this work where the explicit variation of dynamical variables along the Z axis is not amenable to analytical treatment. It can be stated that the enormous post shock thermal pressure in CENBOL is, in reality, capable of providing a substantial amount of ‘hard push’ to the accreting material against the gravitational attraction of the black hole and this ‘thermal kick’ may play an important role in re-distributing the linear momentum of the inflow and generates a non zero component along the Z direction. In other words, thermal pressure at CENBOL, being anisotropic in nature, may deflect a part of inflow along the perpendicular to the equatorial plane of the disc, exact mechanism of which we could not formulate analytically. Thus in our model, the CENBOL successfully connects the two stationary quasi-one dimensional solutions, namely, the 1.5 dimensions vertically averaged inflow and the outflow, to produce a coupled disc-outflow system.

However, we do believe that the CENBOL region is generic (unless viscosity is exorbitantly high which removes angular momentum of the flow almost completely), because all the self-consistent solutions of the governing equations show that angular momentum is almost constant close to the black hole even though the matter start with a large angular momentum at a large (few million) Schwarzschild radius away. As we explained, the viscous time scale is always large compared with the infall time scale, and thus angular momentum remains almost constant and produces the CENBOL. We are not assuming that usual Keplerian disks (farther away) do not form. We think that while forming this Keplerian disk, the angular momentum has been re-distributed and excess has been absorbed by the companion as in the usual scenario. What is new here is the realization that the angular momentum distribution must deviate from a Keplerian distribution close to the black hole and therefore produces a CENBOL closer to the black hole. Such a picture of the inflow with Keplerian flow in the high viscosity region of equatorial plane and low viscosity flow away from it is not due to convenience or necessity, but it arises out of

^{*} By the term ‘ultra-relativistic’ and ‘purely non-relativistic’ we mean a flow with $\gamma = \frac{4}{3}$ and $\gamma = \frac{5}{3}$ respectively, according to the terminology used in Frank et. al (1992).

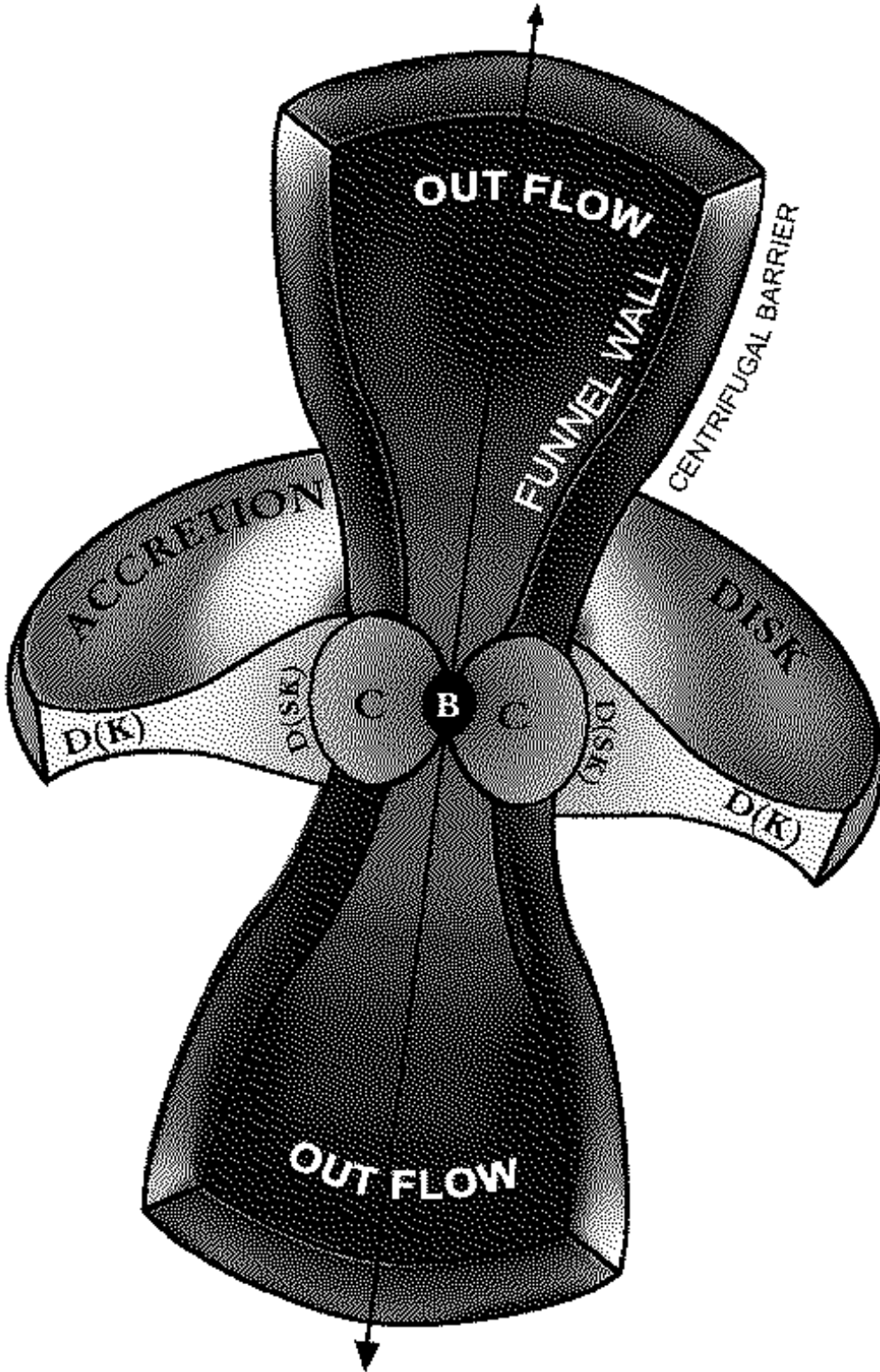


Fig. 2: Multi-component combined flow geometry in 3-Dimension

the actual solutions of the viscous transonic flow equations (see Chakrabarti & Titarchuk 1995 and references therein). This has not only changed our view of the state changes of the black hole spectra (hard/soft), this has also given us clues to the power-law tail of the soft state etc. through the bulk motion Comptonization etc. The interesting feature is that the *same* CENBOL may be responsible for the outflow as well.

There are two surfaces of utmost importance in flows with angular momentum. One is the 'funnel wall' where the effective potential $\Phi_{eff}^i(r)$ vanishes. In the case of a purely rotating flow, this is the 'zero pressure' surface. Flows can not enter inside

the funnel wall because the pressure would be negative. The other surface is called the ‘centrifugal barrier’. This is the surface where the radial pressure gradient of a purely rotating flow vanishes and is located *outside* the funnel wall simply because the flow pressure is higher than zero on this surface. Flow with inertial pressure easily crosses this ‘barrier’ and either enters into a black hole or flows out as winds depending on its initial parameters. It is observed that (DC) the outflow generally hugs the ‘funnel wall’ and goes out in between these two surfaces. Here it is important to note that our assumption of thin inflow is for the sake of computation of the thermodynamic quantities only, but the flow itself need not be physically thin. Also the funnel wall and the centrifugal barrier are purely geometric surfaces, and they exist anyway and the outflow could be supported even by ambient medium which may not necessarily be a part of the disk itself. It is true that the surfaces could have been constructed more accurately if the viscous and other dissipative forces could also be used to obtain this. But the error cannot be high, since the radial motion in the outflow is very small compared to the azimuthal motion at least up to the sonic point.

Qualitatively, one might attempt to ‘visualize’ how the combined accretion-outflow system along with the central accretor would ‘look like’ in reality. In figure 2., we attempt to illustrate the 3-D geometry of coupled disk-outflow system according to our model. **B** is the accreting Schwarzschild black hole while **C**’s represent the hot and dense CENBOL region. **D(K)** and **D(SK)** represent the thin Keplerian part and puffed-up sub-Keplerian part of the advective accretion disk respectively (diagram not in scale). Due to the axisymmetry assumption in accretion, two oppositely directed jet are expelled from the close vicinity of **B**. The inner and the outer surfaces of the outflow are the funnel wall and centrifugal barrier respectively as explained above, see eq. (9a-9b) in next paragraph.

In ordinary stellar mass loss computations, the outflow is assumed to be isothermal till the sonic point (Tarafdar 1988, and references therein). This assumption is probably justified, since copious photons from the stellar atmosphere deposit momenta on the slowly outgoing and expanding outflow and possibly make the flow close to isothermal. This need not be the case for outflows from compact sources. Centrifugal pressure supported boundary layers close to the black hole are very hot (close to the virial temperature) and most of the photons emitted may be swallowed by the black holes themselves instead of coming out of the region and depositing momentum onto the outflow. Thus, the outflows could be cooler than isothermal flows. In our work, we choose polytropic outflows with the same energy as the inflow (i.e., no energy dissipation between the inflow and outflow) but with a different polytropic index $\gamma_o < \gamma$. We have approximated γ_o as a free parameter though in reality γ_o is directly related to the heating and cooling processes of the outflow. However, investigation of such detailed radiative processes are beyond the scope of this work. When \dot{M}_{in} is high, heating of outflow by photon momentum deposition is higher, and therefore $\gamma_o \rightarrow 1$ letting the flow to approach towards its isothermal limit. We also assume that very little viscosity is present in the flow except at the place where the shock forms, so that the specific angular momentum λ is constant in both inflows and outflows close to the black hole. That viscous time scales are longer compared to the inflow time scale, may be a good assumption in the disk, but it may not be a very good assumption for the outflows which are slow prior to the acceleration and are therefore, prone to viscous transport of angular momentum. Such detailed study has not been attempted here particularly because we know very little about the viscous processes taking place in the pre-jet flow. Therefore, we concentrate only those cases where the specific angular momentum is roughly constant when inflowing matter becomes part of the outflow. At the shock, entropy is generated and hence the outflow is of higher entropy for the same specific energy.

For outflow, the energy conservation, mass conservation and the entropy conservation equations can be written as:

$$\mathcal{E} = \frac{v^2}{2} + \frac{a^2}{\gamma_o - 1} + \frac{\lambda^2}{2r_m^2} + \Phi_i(r) \quad (8a)$$

$$\dot{M} = \rho v \mathcal{A}(r) \quad (8b)$$

$$\dot{\mathcal{M}} = a^{\frac{2}{\gamma_o - 1}} v \mathcal{A}(r) \quad (8c)$$

where v is the outflow velocity.

The difference between eq. (3a-3c) and (8a-8c) is that, presently, the rotational energy term contains

$$r_m(r) = \frac{\mathcal{R}(r) + R(r)}{2},$$

as the mean *axial* distance of the flow. The expression of $\mathcal{R}(r)$, the local radius of the centrifugal barrier comes from balancing the centrifugal force with the gravity:

$$\mathcal{R}(r) = \left(\frac{\lambda^2 r}{\Phi'_i(r)} \right)^{\frac{1}{4}} \quad (9a)$$

And the expression for $R(r)$, the local radius of the funnel wall, comes from vanishing of total effective potential, i.e.:

$$R(r) = \lambda \sqrt{\frac{\phi_i(r)}{2}} \quad (9b)$$

so we can write the mean axial distance r_m as:

$$r_m = \frac{1}{2} \left[\lambda \sqrt{\frac{\phi_i(r)}{2}} + \left(\frac{\lambda^2 r}{\Phi'_i(r)} \right)^{\frac{1}{4}} \right] \quad (9c)$$

where $\phi_i(r) = -\Phi_i(r)$. Here, $\mathcal{A}(r)$ is the area between the centrifugal barrier and the funnel wall. This is computed with the assumption that the outflow is external pressure supported, i.e., the centrifugal barrier is in pressure balanced with the ambient medium. Matter, if pushed hard enough, can cross centrifugal barrier in black hole accretion. An outward thermal force (such as provided by the enormous post shock temperature) in between the funnel wall and the centrifugal barrier causes the flow to come out. Thus the cross section of the outflow is,

$$\mathcal{A}(r) = \pi \lambda \left(\frac{\lambda \phi_i(r)}{2} + \sqrt{\frac{r}{\Phi'_i(r)}} \right) \quad (9d)$$

Like accretion, the velocity gradient of the *outflow* can be computed as:

$$\left(\frac{dv}{dr} \right)_i = \frac{\left[\frac{\lambda^3 \phi'_i(r) \sqrt{\frac{2}{\phi_i(r)}} + \left(\frac{r \lambda^{10}}{\Phi'_i(r)} \right)^{\frac{1}{4}} \left(\frac{1}{r} - \frac{\Phi''_i(r)}{\Phi'_i(r)} \right)}{\left[\lambda \sqrt{\frac{\phi_i(r)}{2}} + \sqrt{\lambda} \left(\frac{r}{\Phi'_i(r)} \right)^{\frac{1}{4}} \right]^3} \right] + a^2 \left[\frac{\frac{\lambda \phi'_i(r)}{2} + \frac{1}{2} \sqrt{\frac{r}{\Phi'_i(r)}} \left(\frac{1}{r} - \frac{\Phi''_i(r)}{\Phi'_i(r)} \right)}{\frac{\lambda \phi'_i(r)}{2} + \sqrt{\frac{r}{\Phi'_i(r)}}} \right] - \Phi'_i(r)}{\left(v - \frac{a^2}{v} \right)} \quad (10a)$$

for which the sonic point conditions comes out to be:

$$v_s^i = a_s^i = \sqrt{\left(\frac{\frac{\lambda \phi_i(r)}{2} + \sqrt{\frac{r}{\Phi'_i(r)}}}{\frac{\lambda \phi'_i(r)}{2} + \frac{1}{2} \sqrt{\frac{r}{\Phi'_i(r)}} \left(\frac{1}{r} - \frac{\Phi''_i(r)}{\Phi'_i(r)} \right)} \right)_s \left(\Phi'_i(r) - \frac{\lambda^3 \phi'_i(r) \sqrt{\frac{2}{\phi_i(r)}} + \left(\frac{r \lambda^{10}}{\Phi'_i(r)} \right)^{\frac{1}{4}} \left(\frac{1}{r} - \frac{\Phi''_i(r)}{\Phi'_i(r)} \right)}{\left[\lambda \sqrt{\frac{\phi_i(r)}{2}} + \sqrt{\lambda} \left(\frac{r}{\Phi'_i(r)} \right)^{\frac{1}{4}} \right]^3} \right)_s} \quad (10b)$$

One can solve the following equation to obtain the *outflow* sonic point(s):

$$\begin{aligned} \mathcal{E} - \frac{1}{2} \left(\frac{\gamma_o + 1}{\gamma_o - 1} \right) \left(\frac{\frac{\lambda \phi_i(r)}{2} + \sqrt{\frac{r}{\Phi'_i(r)}}}{\frac{\lambda \phi'_i(r)}{2} + \frac{1}{2} \sqrt{\frac{r}{\Phi'_i(r)}} \left(\frac{1}{r} - \frac{\Phi''_i(r)}{\Phi'_i(r)} \right)} \right)_s \left(\Phi'_i(r) - \frac{\lambda^3 \phi'_i(r) \sqrt{\frac{2}{\phi_i(r)}} + \left(\frac{r \lambda^{10}}{\Phi'_i(r)} \right)^{\frac{1}{4}} \left(\frac{1}{r} - \frac{\Phi''_i(r)}{\Phi'_i(r)} \right)}{\left[\lambda \sqrt{\frac{\phi_i(r)}{2}} + \sqrt{\lambda} \left(\frac{r}{\Phi'_i(r)} \right)^{\frac{1}{4}} \right]^3} \right)_s \\ + \frac{\lambda}{\left[\sqrt{\frac{\lambda \phi_i(r)}{2}} + \left(\frac{r}{\Phi'_i(r)} \right)^{\frac{1}{4}} \right]^2 + \Phi'_i} = 0 \end{aligned} \quad (10c)$$

and the outflow velocity gradient at the sonic point(s) can be obtained by solving the following equation:

$$\begin{aligned} \left(\frac{2\gamma_o - 1}{\gamma_o - 1} \right) \left(\frac{dv}{dr} \right)_s^2 + 2a_s(\gamma_o - 1) \left[\frac{\frac{\lambda \phi'_i(r)}{2} + \frac{1}{2} \sqrt{\frac{r}{\Phi'_i(r)}} \left(\frac{1}{r} - \frac{\Phi''_i(r)}{\Phi'_i(r)} \right)}{\frac{\lambda \phi'_i(r)}{2} + \sqrt{\frac{r}{\Phi'_i(r)}}} \right]_s \left(\frac{dv}{dr} \right)_s - \\ \frac{1}{\pi \lambda} \left(\frac{a}{\frac{\lambda \phi_i(r)}{2} + \sqrt{\frac{r}{\Phi'_i(r)}}} \right)_s^2 \left[\frac{\lambda \Phi'_i(r)}{2} - \frac{1}{2} \left(r \Phi'_i(r) \right)^{-\frac{1}{2}} \left(\frac{1}{r} + \frac{1}{2} \frac{\Phi''_i(r)}{\Phi'_i(r)} \right) - \frac{1}{2} \sqrt{\frac{r}{\Phi'_i(r)}} \frac{\Phi''_i(r)}{\Phi'_i(r)} \left(\frac{1}{2r} - \frac{1}{3} \frac{\Phi''_i(r)}{\Phi'_i(r)} \right. \right. \\ \left. \left. + \frac{\Phi'''_i(r)}{\Phi''_i(r)} \right)_s - (\gamma_o - 1) \left[\frac{\frac{\lambda \phi'_i(r)}{2} + \frac{1}{2} \sqrt{\frac{r}{\Phi'_i(r)}} \left(\frac{1}{r} - \frac{\Phi''_i(r)}{\Phi'_i(r)} \right)}{\frac{\lambda \phi'_i(r)}{2} + \sqrt{\frac{r}{\Phi'_i(r)}}} \right]_s^2 + \frac{3}{4} \lambda^2 \frac{\left[\lambda \phi'_i(r) \sqrt{\frac{2}{\phi_i(r)}} + \left(\frac{\lambda^2 r}{\Phi'_i(r)} \right)^{\frac{1}{4}} \left(\frac{1}{r} - \frac{\Phi''_i(r)}{\Phi'_i(r)} \right) \right]_s^2}{\left[\lambda \sqrt{\frac{\phi_i(r)}{2}} + \left(\frac{\lambda^2 r}{\Phi'_i(r)} \right)^{\frac{1}{4}} \right]_s^4} \right. \\ \left. - \frac{8\lambda^2}{\left[\lambda \sqrt{\frac{\phi_i(r)}{2}} + \left(\frac{\lambda^2 r}{\Phi'_i(r)} \right)^{\frac{1}{4}} \right]_s^3} \left[2\lambda \phi'_i(r) \sqrt{\frac{2}{\phi_i(r)}} \left(\frac{\phi''_i(r)}{\phi'_i(r)} - \frac{1}{2} \frac{\phi'_i(r)}{\phi_i(r)} \right) + \frac{1}{r} \left(\frac{\lambda^2 r}{\Phi'_i(r)} \right)^{\frac{1}{4}} \left(\frac{1}{3r} - \frac{1}{4r} \frac{\phi''_i(r)}{\phi'_i(r)} \right) - \right. \right. \\ \left. \left. \frac{\phi''_i(r)}{\phi'_i(r)} \left(\frac{\lambda^2 r}{\Phi'_i(r)} \right)^{\frac{1}{4}} \left(\frac{\phi'''_i(r)}{\phi''_i(r)} - 5 \frac{\phi''_i(r)}{\phi'_i(r)} - \frac{1}{4r} \right) \right]_s + \Phi''_i(r) \right]_s = 0 \end{aligned} \quad (10d)$$

The mass outflow rate $R_{\dot{m}}$ can now be defined as:

$$R_{\dot{m}} = \frac{\dot{M}_{out}}{\dot{M}_{in}} = \Psi(\mathcal{E}, \lambda, \gamma, \gamma_o) \quad (11)$$

where Ψ has some complicated non-linear non-linear functional form which can *not* be evaluated analytically.

The following procedure is adopted to obtain a complete solution of the coupled accretion-outflow system. For any $[\mathcal{P}_i] \in \mathbf{PTR}$ (see Fig. 1), suppose that matter first enters through the outer sonic point and passes through a shock. At the shock, part of the incoming matter, having higher entropy density is likely to return back as winds through a sonic point, other than the one it just entered. That is because, since the outflow would be heated by photons, and thus have a smaller polytropic constant, the flow would leave the system through an outer sonic point different from that of the incoming solution. Thus a combination of topologies, one from the region **PTR**, and the other corresponding to the flow with same $(\mathcal{E}_i, \lambda_i)$ but now with $\gamma = \gamma_o$, are required to obtain a full solution. Thus finding a complete self-consistent solution boils down to finding the outer sonic point of the outflow and the mass flux through it. A supply of parameters \mathcal{E} , λ , γ and γ_o make a self-consistent computation of $R_{\dot{m}}$ possible. We obtain the inflow sonic point by solving Eq. (4c). From Eq. (41-4d), using the fourth order Runge Kutta method, $u(r)$, $a(r)$ and the inflow Mach number $\left[\frac{u(r)}{a(r)}\right]$ are computed along with the inflow from the *inflow* sonic point till the position where the shock forms. The shock location is calculated by solving Eq. (5). Various shock parameters (i.e., density, pressure etc at the shock surface) are then computed self-consistently. For outflow, with the known value of \mathcal{E}, λ and γ_o , it is easy to compute the location of the outflow sonic point from Eq. (10c). At the outflow sonic point, the outflow velocity v_s^i and polytropic sound velocity a_s^i is computed from Eq. (10b). Using Eq. (10a) and (10d), $(\frac{dv}{dr})$ and $(\frac{da}{dr})_s$ is computed as was done for the inflow. Runge -Kutta method is then employed to integrate from the *outflow* sonic point towards the black hole to find out the outflow velocity and density at the shock location for a given accretion rate and \dot{M}_{out} is calculated from Eq. (8b). The mass outflow rate $R_{\dot{m}}$ is then computed using Eq.(11) and the corresponding ν_{QPO} is computed using Eq. (7). As Φ_1 is the best available potential to mimic the general relativistic results for multi-transonic shocked accretion, we will calculate ν_{QPO} and $R_{\dot{m}}$ only for flows in Φ_1 by setting:

$$[\Phi_i(r), \Phi'_i(r), \Phi''_i(r), \Phi'''_i(r),] \Rightarrow [\Phi_1(r), \Phi'_1(r), \Phi''_1(r), \Phi'''_1(r),]$$

while simultaneously solving equations (2-11), using the procedure described above. One may ask the question that if we plan to explore the $\nu_{QPO} - R_{\dot{m}}$ correlation only for $\Phi_1(r)$, why then we formulate all the equations for all $\Phi_i(r)$ s in general instead of $\Phi_1(r)$, which would be a relatively less complicated procedure. Our answer to this question is mainly two-fold. Firstly, we wanted to present a generalized formulation for *all* $\Phi_i(r)$ s to get convinced that such correlation can be theoretically investigated for *any* kind of black hole potential and to assure that our model is *not* just an artifact of a particular type of potential only. Secondly, of course there are possibilities that in future someone may come up with a pseudo-Schwarzschild potential better than $\Phi_1(r)$, which will be the best approximation for complete general relativistic investigation of multi-transonic shocked flow. In such case, if one can in advance formulate a generalized model for coupled accretion-wind system for any arbitrary $\Phi_i(r)$, exactly what we have done in this paper, then that generalized model will be able to readily accommodate that new $\Phi(r)$ without having any significant change in the fundamental structure of the formulation and solution scheme of the model and we need not have to worry about providing any new scheme exclusively valid only for that new potential, if any. Thus we believe that our general inflow-outflow model presented in this paper, which bears the same philosophy as provided by D98 and DC but treats the problem in a much more general way, will be quite useful for any further improvement in this field and our theoretical correlation study can also be extended easily for any such new and more accurate potential that might be discovered in future. It is to be noted that we cannot accelerate any matter more than the sound speed (or, the rotational velocity) at the initial injection point so we do not claim to explain superluminal motions. We have done what is hydrodynamically possible. If we follow our path for MHD flows, we believe that we could reach superluminal motions also. Also, we could not do a thorough job on angular momentum distribution *inside* the jet. What we understand here is that in case, some form of viscosity is working (say radiative viscosity) inside the jet to make the distribution of the angular momentum as a power-law, then the resulting density will go up towards the edge of the jet (a ‘hollow’ jet as in Hawley, Smarr & Wilson 1984, for example). Thus, since maximum amount of matter is taking away maximum amount of angular momentum (unlike in the disc), the average angular momentum need not be different from that of the CENBOL region. But in case, the average angular momentum were lower, then we find that the outflow rate was also lower.

In Fig. 3, we represent our theoretical results regarding the correlation of ν_{QPO} with $R_{\dot{m}}$. We define the normalized QPO frequency f_{norm} in the following way:

$$f_{norm} = \frac{\nu}{\nu_{max}} \quad (12)$$

where $\nu = \nu_{QPO}$ is the theoretically calculated QPO frequency obtained from eqn. (7), with properly scaled C and ν_{max} is the highest possible observed frequency for any particular astrophysical source. This normalization is necessary because exact value of C in the equation cannot be estimated analytically. We plot f_{norm} along the X axis and the mass outflow rate scaled in solar mass per year is plotted along the Y axis. We calculate the ν_{QPO} as well $R_{\dot{m}}$ for such shocked ultra-relativistic accretion on to a $10 M_{\odot}$ black hole at unit Eddington rate \dot{M}_{Edd} . The value of \mathcal{E} and λ for which the calculation is performed are taken from the region **PTR** of Fig. 1. The scheme for the calculation is the following:

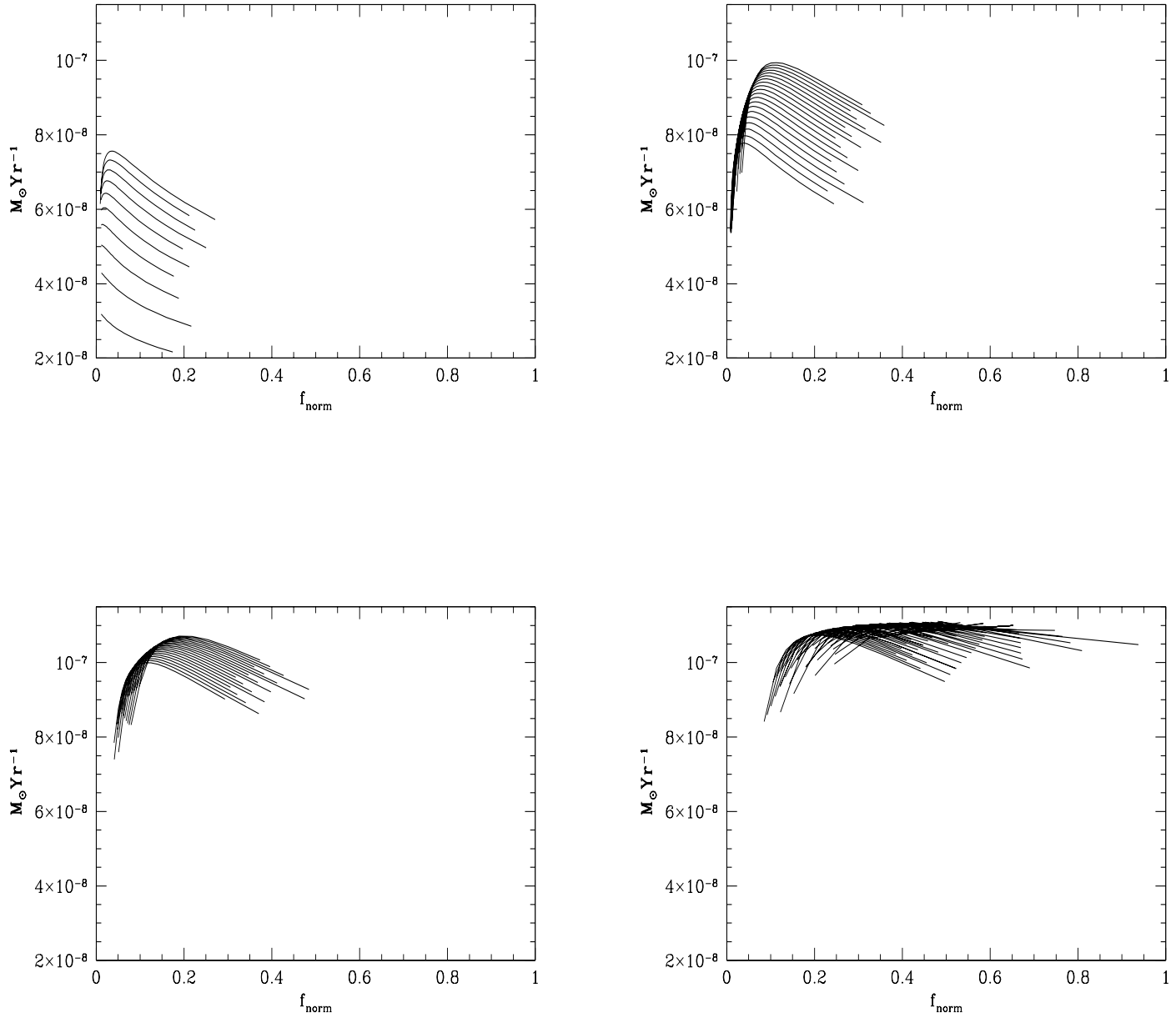


Fig. 3 Correlation among the QPO frequencies and the mass outflow rates for coupled accretion-wind system in $\Phi_1(r)$. $f_{\text{norm}} = \frac{\nu}{\nu_{\text{max}}}$ is the normalized dimensionless QPO frequency which is basically the ratio of the theoretically calculated QPO frequencies to the highest possible observed QPO frequency for any particular astrophysical source, see text for detail.

First we calculate shock location r_{sh} , shock compression ratio R_{comp} and consequently the QPO frequency ν_{QPO} for the fixed lowest possible \mathcal{E} with the range of λ for which the shock forms. We also calculate R_m for this set of parameters. We then repeat this calculation for higher values of energy till all \mathcal{E} and λ covering the region **PTR** are exhausted.

Fig. 3 is divided into four blocks. Each individual curve in any block represents the variation of f_{norm} on R_m resulted from the variation of λ by keeping \mathcal{E} fixed, and different curves are drawn for different \mathcal{E} with $\Delta\mathcal{E} = 10^{-3}$. As stated earlier, \mathcal{E} and λ covering the region **PTR** are used to draw Fig. 3. The whole range of specific energy of the shocked accretion material for which computation is done, was divided into four parts. The top left block represents results from very low energy accretion, top right for medium energy accretion, bottom left for moderately high energy accretion and bottom right is for very high energy accretion. One can observe that for very low energy accretion, normalized QPO frequency non-linearly and monotonically anti-correlates with the mass outflow rate and the calculated ν_{QPO} is also relatively low. As the specific energy of the accreting material increases, a peak appears in the correlation curve and the monotonic behavior is not maintained

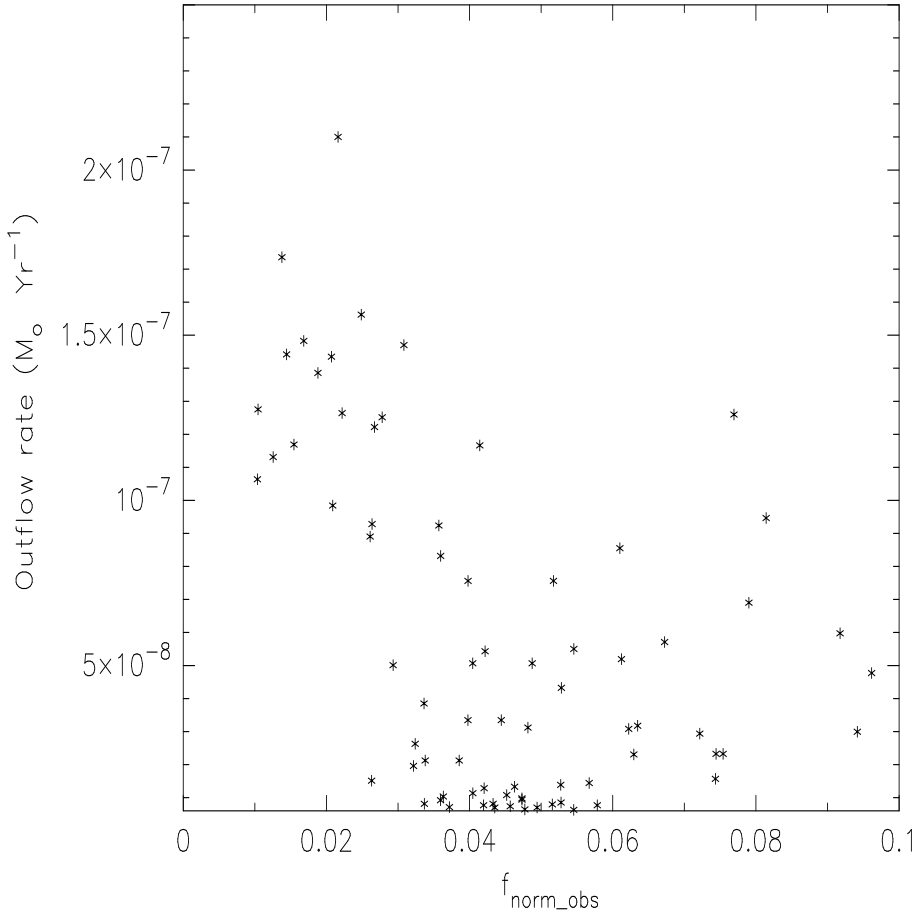


Fig. 4: The outflow rate plotted against normalized QPO frequency for GRS 1915+105, as calculated from the observed radio flux and the measured QPO frequency.

anymore. As \mathcal{E} becomes higher, the normalized QPO frequency first non-linearly correlates with the mass outflow rate up to a certain value of ν_{QPO} (or with f_{norm}) for which the mass loss rate becomes maximum, then the anti-correlation phase starts like low energy accretion cases.

It is to be noted here that both f_{norm} as well as $R_{\dot{m}}$ depend on initial boundary conditions and are quite sensitive to the shock location r_{sh} . While f_{norm} non-linearly and monotonically anti-correlates with r_{sh} , one can show that $R_{\dot{m}}$ represents a distinctive non-monotonic variation with r_{sh} . When shock location is small, $R_{\dot{m}}$ non-linearly correlates with r_{sh} and attains a peak at a particular value of r_{sh} , say at r_{sh}^p . For $r_{sh} > r_{sh}^p$ (if available for a set of initial boundary condition), $R_{\dot{m}}$ starts anti-correlating with r_{sh} . These informations might be used in the following way to infer whether our calculation is model dependent or not.

For the same set of initial boundary conditions, the shock location distinctively differs for various Φ_i used here. This is because of the fact that the region of parameter space (spanned by \mathcal{E} , λ and γ) responsible for shock formation is quite different for almost all four Φ_i (see Fig. 4 and Fig. 7 of D02). Hence for a particular value of $[\mathcal{P}_i]$, one obtains *numerically different* value of f_{norm} and $R_{\dot{m}}$ for all Φ_i in general. This information, by any means, does *not* imply that our calculation is model dependent[†] because though the numerical values may differ, the overall $f_{norm} - R_{\dot{m}}$ (anti) correlation profile *does* remain the same for all Φ_i . This is because of the fact that $f_{norm} - r_{sh}$ anti-correlation and $R - \dot{m} - r_{sh}$ (anti) correlation profile remains unaltered for all Φ_i s, only the numerical values of the related quantities change with the choice of potential. Thus we may, perhaps, conclude that our calculation is more or less ‘generalized’ in nature to include all existing pseudo-Schwarzschild potentials.

[†] By the term ‘model (in) dependent; we mean whether the basic physics remains unaltered or drastically changes with a specific choice of Φ_i .

4 COMPARISON WITH OBSERVATIONS

The Galactic microquasar GRS 1915+105 shows several properties which are indicative of the existence of shock oscillations in terms of QPOs and collimated jets in terms of radio emission (see Belloni 2002 for a general review on this particular source). Since it has showed intense and highly variable X-ray and radio emission characteristics, it has been extensively studied and it is an ideal source to test our concepts on shock oscillations and outflows.

GRS 1915+105 shows diverse variability characteristics (see Belloni et al. 2000a for a classification) and the inter-relationship between these variability classes and the radio emission has been examined in detail (Naik & Rao 2000; Belloni et al. 2000b; Muno et al. 2001; Rao et al. 2000). Highly variable steep spectrum radio emission are invariably associated with superluminally moving ejecta and these are causally connected to a disturbed accretion disc as observed in X-rays as some sort of ‘inner disk oscillations’. These events could be initiated by some catastrophic events like the ‘magnetic rubber band’ effect (Nandi et al. 2001). Steady flat spectrum radio emission, on the other hand, is always associated with the hard X-ray state of GRS 1915+105 and one of the identifying feature of such hard states is the existence of an ubiquitous 0.5 – 10 Hz QPO (Muno et al. 2001). It would be quite instructive to compare our results obtained in the previous sections to the outflow properties (as observed in radio) and shock oscillation properties (measured as the 0.5 – 10 Hz QPO) of GRS 1915+105.

When the outflow is confined to the outer sonic point in the wind, the material can get collected and after some time can cause a catastrophic Compton cooling. This concept has been successfully used by CM to explain the repeated variation between high and low states in GRS 1915+105 and a relation between the QPO frequency and the ‘low-state’ (or ‘off’ state) duration has been derived and compared with the observations. Based on this concept, we can relate the predicted QPO frequency to the observed one by scaling to the maximum observed QPO frequency of 67 Hz (Morgan et al. 1997).

To convert the observed radio luminosity to outflow rate, we adapt the method given in Fender & Pooley (2000). We assume that the radio spectrum has a flat spectrum from 1 GHz to 1.4×10^5 Hz (corresponding to mid-IR region of $2.3\mu\text{m}$) and get a conversion factor of observed radio flux to jet luminosity as 1.35×10^{35} erg s $^{-1}$ per mJy (for a distance of 12.5 kpc). The jet luminosity, L_J , can be converted to jet power, P_J by

$$P_J \sim L_J \eta^{-1} F(\Gamma, i) \quad (13)$$

where η is the radiative efficiency and $F(\Gamma, i)$ is the correction factor for bulk motion (see Fender & Pooley 2000). $\eta^{-1} F(\Gamma, i)$ has a typical value of 10. Further assuming that the jet emitting region has a typical volume of 10^{40} cm 3 and a magnetic field of 100 G, we can convert the jet power to outflow rate, getting a conversion factor of $1.4 \epsilon \times 10^{-8} M_\odot \text{ yr}^{-1}$ per 1 mJy for GRS 1915+105, where ϵ is the fraction of particles accelerated to relativistic energies. In our present work, we have calculated the total outflow and further acceleration, presumably in some shock regions in the jet, would be required to accelerate these particles to relativistic energies. Since our purpose in the present work is only to get an estimate of the relative variation of outflow rate to shock oscillations, we have taken a conservative value of 0.1 for ϵ .

Using these conversion factors, we have plotted the observed outflow rate as a function of normalized QPO frequency, $f_{\text{norm-obs}}$ in Figure 4, based on a compilation by Muno et al. (2001). It should be noted that there is a general agreement with the trend of observations as predicted by the theory (see Figure 3) in the sense that the outflow rate shows an increase with f_{norm} at low frequencies, reaches a maximum, and then slowly declines. The agreement, however, is particularly close for the case of low specific energy (Figure 3, top left). The QPOs seen in GRS 1915+105 pertains to the steady low-hard states where the accreted matter can steadily loose its energy till it reaches the CENBOL and the specific energy can be very low for the accreting matter close to the black hole. The system can go into a high specific energy accretion mode at certain occasions (for example during the infrequent times when the high frequency - 67 Hz - QPOs are seen). It would be interesting to steady the behavior of QPO frequency and the outflow rate during such modes and we speculate that the variations would look more like the high specific energy behavior (Figure 3, bottom right). Also, there are possibilities that the outflowing matter (the ejecta) is essentially dominated by low binding energy (because they are supposed to be escaped towards infinity), hence such correlation in stronger for low energy accretion. We must, however, caution that there are several uncertainties in the derivation of the outflow rate from the observed radio luminosity, but, the connection between the radio emission and the properties of the accretion disc seems to be on the line predicted by the Advective Flow formalism, described in detail in this paper. A detailed simultaneous observations and a calculation of the X-ray spectra using proper hydrodynamic formalisms would be required to further refine the model predictions.

It is worth pointing out that the total amount of outflow observed in GRS 1915+105 during the ‘baby-jet’ episodes as well as during the super-luminal jet emission are also consistent with calculations presented here. Multi-wavelength observations of GRS 1915+105 (Mirabel et al. 1998) showed evidence for a blob of matter being ejected out, which are called the ‘baby-jets’, and it is estimated that $> 10^{19}$ g of matter is ejected during these events. It was pointed out by Belloni et al. (2000a) that these events are always preceded by hard dips characterized by ~ 3 Hz QPOs and they hypothesis that the matter for jet emission is ejected during these hard dips lasting for ~ 500 s. Hence, a mass outflow of $\sim 10^{-10} M_\odot \text{ yr}^{-1}$ must be participating in the relativistically accelerated particles, which is about 1% of the outflow estimated in our calculations. GRS 1915+105 also shows superluminal jet emission with an estimated total mass of 10^{23} g (Mirabel & Rodriguez 1999; Fender et al. 1999). These events could be either due to a series of dips preceded by low hard states with QPO frequency ~ 1 Hz (Naik et al. 2001) or due to the accumulation of matter during an enhanced low state lasting for a few days (Dhawan et al. 2000). In either case, there is evidence that the ejected matter is accumulated during the low hard state with equivalent f_{norm} of 0.01 and lasting for $\sim 50,000$ s giving an effective outflow rate of $10^{-8} M_\odot \text{ yr}^{-1}$, consistent with the calculation presented here.

5 CONCLUDING REMARKS

In this paper we attempt to calculate the QPO frequency of the central accretor harbored by the galactic microquasar sources and to explore the dependence of the amount of baryonic load in the microquasar jets on these frequencies. Our calculation has been performed for *polytropic* shocked accretion onto galactic stellar mass black holes using a generalized post-Newtonian pseudo-Schwarzschild framework. However, one can show that shock formation is also possible when accretion is taken to be *isothermal* (Das, Pendharkar & Mitra 2003), and it is possible to calculate the normalized QPO frequencies for such accretion flow as well (Das 2003). In our future work, we would like to explore the correlation between ν_{QPO} and R_m for shocked isothermal inflow as mentioned above.

Theory of accretion onto black holes is inherently a tough and intractable problem: first of all the nature of viscosity which is known to be turbulent even in mildly relativistic accretion flows is difficult to even formulate, let alone solve, in the relativistic accretion flows likely to be present in these system and the inner boundary condition is impossible to formulate and analytically handle in regions where general theory of relativity is known to predominate. The approach that we have taken in this work is the one in which general theory of relativity is handled in a set of pseudo-Schwarzschild potentials and the solutions are sought in regimes close to the black hole where the flow is shown to be supersonic and likely to be inviscid. Two fundamental problems are inherent in this approach namely:

- 1) How are we sure that the pseudo-Schwarzschild potentials give correct description of general theory of relativity, and
- 2) How do we extrapolate the results from inner regions of accretion disc where the accretion is likely to be inviscid to the outer regions where the flow is viscous and most of the observables like X-ray emission characteristics are measurable.

We understand that such questions cannot be answered with mathematical certainty, but the present paper takes very important steps in that direction. By showing that shocks exist in all available pseudo-Schwarzschild potentials we have increased the confidence that shocks should indeed exist in the correct general relativistic formalism. By carefully selecting some important observables which are likely to be the manifestations of the conditions of inner accretion disk, we have attempted to make a semi-qualitative comparison with the theoretical predictions and have obtained very encouraging results. Though the fundamental problem of obtaining a complete solution for accretion onto black holes is not solved, very important insights are obtained in the present work which increases the confidence in the methodology and detailed prescriptions are given for comparison with observations.

6 ACKNOWLEDGEMENTS

This research has made use of NASA's Astrophysics Data System Bibliographic Services. Research of TKD at UCLA is supported by NSF funded post doctoral fellowship (Grant No. NSF AST-0098670). TKD would like to acknowledge the hospitality provided by the Racah Institute of Physics, The Hebrew University of Jerusalem, Israel, where a part of this work had been done. He would also like to acknowledge the hospitality provided by the Department of Astronomy and Astrophysics, Tata Institute of Fundamental Research, where he used to visit frequently to work with the members of the X-Ray Astronomy Group. The authors would like to thank the anonymous referee for a number of useful comments.

REFERENCES

Artemova, I. V., Björnsson, G., & Novikov, I. D. 1996, ApJ, 461, 565 (ABN)
 Begelman, M. C., Blandford, R. D., & Rees, M. J. 1984, Rev. Mod. Phys. 56, 255
 Belloni, T. 2002, Proc. of the 4th Microquasar Workshop, eds. Ph Durouchoux, Y. Fuchs and J. Rodriguez (Center for Space Physics: Kolkata), astro-ph/0208129
 Belloni, T., Klein-Wolt, M., Mendez, M., et al., 2000a, A&A, 355, 271
 Belloni, T., Migliari, S., & Fender, R. P. 2000b, A&A, 358, L29
 Chakrabarti, S. K. & Manickam, S. G. 2000, ApJ, 531, L41
 Chakrabarti, S. K., & Titarchuk, L. G. 1995 ApJ, 455, 623
 Das, T. K. 1998, in Observational Evidence for Black Holes in the Universe, Ed. S. K. Chakrabarti (Kluwer Academic: Holland), p. 113 (D98)
 Das, T. K. 2001, ApSSS, 276, 267 267-272
 Das, T. K. 2002, ApJ, 577, 880 (D02)
 Das, T. K. 2003, ApJ Letters. To Appear in Vol. 588, May 10 Issue (astro-ph/0302014)
 Das, T. K., & Chakrabarti, S. K. 1999, Class. Quantum Grav, 16, 3879 (DC)
 Das, T. K., & Sarkar, A. 2001, A & A, 374, 1150
 Das, T. K., Pendharkar, J., & Mitra, S. 2003, ApJ, To Appear in Vol. 592, 1st Aug. Issue. (astro-ph/0301189)
 Dhawan, V., Mirabel, I.F. & Rodriguez, L.F. 2000, ApJ, 543, 373
 Fender, R. P., & Pooley, G. G. 2000, MNRAS, 318, L1
 Fender, R. P., Garrington, S. T., McKay, D. J., Muxlow, T. W. B., Pooley, G. G., Spencer, R. E., Stirling, A. M., & Waltman, E. B. 1999, MNRAS, 304, 865
 Ferrari, A. 1998, ARA&A
 Frank, J., King, A., & Raine, D. 1992, Accretion Power in Astrophysics. 2nd. Edition. Cambridge University Press.
 Hawley, J. F.; Wilson, J. R.; & Smarr, L. L. 1984, ApJ, 277,296

Landau, L. D., & Lifshitz, E. D. 1959, *Fluid Mechanics* (New York: Pergamon)
Mirabel, I. F., & Rodriguez, F. L. 1999, *ARA&A*, 37, 409
Morgan, E. H., Remillard, R. A., & Greiner, J. 1997, *ApJ*, 482, 993
Muno, M. P., Morgan, E. H., & Remillard, R. A. 1999, *ApJ*, 527, 321
Muno, M. P., Remillard, A., Morgan, E. H., Waltman, E. B., Dhawan, V., Hjellming, R. M., Pooley, G. G. 2001, *ApJ*, 556, 515
Nandi, A., Chakrabarti, S. K., Vadawale, S. V. & Rao, A. R. 2001, *A&A*, 380, 245
Naik, S. & Rao, A.R. 2000, *A&A*, 362, 691
Naik, S., Agrawal, P. C., Rao, A. R., Paul, B., et al. 2001, *ApJ*, 546, 1075
Paczynski, B. & Wiita, P. J. 1980, *A & A*, 88, 23
Nowak, A. M., & Wagoner, R. V. 1991, *ApJ*, 378, 656
Rao, A. R., Yadav, J. S. & Paul, B. 2000, *ApJ*, 544, 443
Rutledge, R. E. et al. 1999, *ApJ Suppl. Ser.*, 124, 265
Shakura, N. I., & Sunyaev, R. A. 1973, *A & A*, 24, 337
Shrader, C. R., & Titarchuk, L. G. 1998, *ApJ*, 499, L31
Smith, D. M., Heindl, W. A., & Swank, J. H. 2001 (astro-ph/0103304)
Tarafdar, S.P. 1988, *Ap.J.*, 331, 932
Titarchuk, L., Lapidus, I., & Muslimov, A. 1998, *ApJ*, 499, 315
Webb, W., & Malkan, M. 2001, *ApJ*, 540, 652